A Unified Approach to Cooperative and Non-Cooperative Sense-and-Avoid

Subramanian Ramasamy and Roberto Sabatini
School of Aerospace, Mechanical and Manufacturing Engineering
RMIT University, Melbourne, VIC 3000, Australia
roberto.sabatini@rmit.edu.au

***Abstract*—Cooperative and non-cooperative Sense-and-Avoid (SAA) capabilities are key enablers for Unmanned Aircraft Vehicle (UAV) to safely and routinely access all classes of airspace. In this paper state-of-the-art cooperative and non-cooperative SAA sensor/system technologies for small-to-medium size UAV are identified and the associated multi-sensor data fusion techniques are introduced. A reference SAA system architecture is presented based on Boolean Decision Logics (BDL) for selecting and sorting non-cooperative and cooperative sensors/systems including both passive and active Forward Looking Sensors (FLS), Traffic Collision Avoidance System (TCAS) and Automatic Dependent Surveillance – Broadcast (ADS-B). After elaborating the SAA system processes, the key mathematical models associated with both non-cooperative and cooperative SAA functions are presented. The analytical models adopted to compute the overall uncertainty volume in the airspace surrounding an intruder are described. Based on these mathematical models, the SAA Unified Method (SUM) for cooperative and non-cooperative SAA is presented. In this unified approach, navigation and tracking errors affecting the measurements are considered and translated to unified range and bearing uncertainty descriptors, which apply both to cooperative and non-cooperative scenarios. Simulation case studies are carried out to evaluate the performance of the proposed SAA approach on a representative host platform (AEROSONDE UAV) and various intruder platforms. Results corroborate the validity of the proposed approach and demonstrate the impact of SUM towards providing a cohesive logical framework for the development of an airworthy SAA capability, which provides a pathway for manned/unmanned aircraft coexistence in all classes of airspace.**

Keywords—Unamnned Aircraft Vehicle; Sense-and-Avoid; Unified Approach; Cooeprative; Non-Cooperative; Sensors.

I. INTRODUCTION

The integration of Unmanned Aircraft Vehicle (UAV) into all classes of airspace involves a series of challenges in order to ensure safe operations [1]. Unmanned Aircraft Systems (UAS) are becoming to be used for a number of civilian and military applications, although the enabling technologies are considered to be far less developed in maturity level when compared to that of manned aircraft, raising concerns to the certification authorities, airspace users as well as general public [2]. One of the main challenges is the implementation of a unified approach to both non-cooperative and cooperative Sense-And-Avoid (SAA), which enables RPAS to perform equally or exceed the performance of the see-and-avoid ability of the pilot in manned aircraft [3]. A SAA system installed on a UAS should be capable of operating under various weather conditions and situations [4] and, as autonomy increases, with limited operator involvement. This entails information fusion from multiple sensors [2]. The SAA capability is defined as the automatic detection of possible conflicts by the UAV platform under consideration, resolving the collision risks and performing optimised avoidance manoeuvre tasks to prevent the identified collisions. In this context, the fundamental areas that need to be addressed for integrating UAVs in commercial airspace/aerodromes have been identified as part of the Aviation System Block Upgrades (ASBU) by the International Civil Aviation Organization (ICAO) [5]. Initial integration is envisaged by implementation of basic procedures and functions including that of SAA functions. Integration of UAVs in airspace traffic is foreseen by the implementation of refined procedures that would also cover lost links as well as enhanced SAA functions with higher degree of automation and meeting the required levels of integrity. Finally, UAV transport management will involve the implementation of UAV operations on the airport surface and in commercial airspace similar to conventionally piloted aircraft. In the Communication, Navigation and Surveillance/Air Traffic Management (CNS/ATM) and avionics (CNS+A) context, the first recommendation addressing the operational and certification issues for civil UAS was issued by the Joint Aviation Authorities (JAA) CNS/ATM Steering Group [6, 7]. Subsequently, the EUROCAE Working Group (WG-73) endeavours to address the following aspects:

- UAV operations enabled by cooperative and non-cooperative SAA solutions.
- Command, control, communication, spectrum and security issues.
- Initial and continued airworthiness.

Current advances in state-of-the-art airborne sensors and multi-sensor data fusion methods have led to a number of innovative but at the same time dispersed non-cooperative and cooperative SAA solutions. Non-cooperative Collision Detection and Resolution (CD&R) for UAVs is considered as one of the key challenges that needs to be addressed. As a result, a number of non-cooperative sensors have been adopted as part of the research projects dealing with developing SAA functions. Multi-sensor platforms for obstacle detection by using millimetre-wave radar, electro-optic/infrared, Light Detection and Ranging (LIDAR) and

acoustic sensors are currently employed [8-10]. Ground-based SAA systems using electronic sensors are adopted and they provide information for supporting decision tasks especially in Terminal Manoeuvring Area (TMA) operations. Light Detection and Ranging (LIDAR) is used for detecting, tracking and avoiding obstacles in low-level flight [10]. The adoption of a multi-sensory approach to SAA (employing passive and active MMW radar, Forward Looking Infra-Red (FLIR), LIDAR and an Electronic Surveillance Module (ESM) for obstacle detection) has resulted in adequate performance in low- to medium-dynamics platform applications. Synthetic Aperture Radar (SAR) equipped in a UAV platform is adopted for detecting motion and also in determining location, velocity, and size of ground obstacles [8]. Acoustic-based SAA system for small RPAS by adopting a multi sensor platform with acoustic sensors that allows detection of obstacles and intruders in a 360º Field of View (FOV) and by performing quick-reaction manoeuvres for avoidance has proved to be effective [11]. An approach to the definition of encounters models and their applications on the SAA strategies take into account both cooperative and non-cooperative scenarios. The states of the tracked obstacles are obtained by adopting Extended/Unscented Kalman Filter (EKF/UKF), particle filter or other multi-senor data fusion techniques including learning based mechanisms is used in order to predict the trajectory in a given time horizon. On-board trajectory re-planning with dynamically updated constraints based on the intruder and the host dynamics is at present used to generate obstacle avoidance trajectories [12]. In the case of Cooperative scenarios, Automatic Dependent Surveillance–Broadcast (ADS-B) and Traffic Collision Avoidance System (TCAS) are adopted for implementing SAA [13]. Coarse-resolution radar based SAA solution has been implemented for small size UAVs [14] and its information is fused with data from ADS-B [15]. The avoidance trajectory is generated considered the use of on-board trajectory re-planning module with dynamically updated constraints based on the intruder and the host dynamics. The avoidance trajectories are also generated by considering the use of a nonlinear differential geometric guidance law based on collision cone approach and dynamic inversion, which, combined with a first order autopilot, allows for a satisfactory guidance of the UAV. As part of this research, the possible synergies attainable with the adoption of different detection, tracking and trajectory avoidance algorithms are studied. Additionally, a unified approach to cooperative and non-cooperative SAA is developed by determining the overall uncertainty volume in the airspace surrounding the intruder tracks.

II. Sensor Technologies

The requirements for designing and developing an effective SAA system are derived from the current regulations applicable for the see-and-avoid capability of manned aircraft [16-18]. The proposed detection range and Field of Regard (FOR) have to be adequate to ensure separation from the intruder to prevent a probable near mid-air collision. In the case of see-and-avoid, the main roles and responsibilities of pilots and human factors are stated in FAA AC 90-48C and FAR 91.113 regulations as vigilance shall be maintained at all times, regardless of whether the operation is conducted under Instrument Flight Rules (IFR) or Visual Flight Rules (VFR). Novel Human Machine Interface (HMI) engineering designs specifically targeting SAA capability are proposed as part of the US Air Force Common Airborne Sense and Avoid (C-ABSAA) program [19]. One of the fundamental limitations for certification authorities to fully certify SAA is to evaluate the ability of the current and future UAVs to be able to replicate the human see-and-avoid capability, at a comparable or superior level upon replacing the on-board pilot with a Ground Control Station (GCS) operator. The currently available SAA technologies do not meet the targeted levels of safety with the practical Size, Weight and Power (SWaP) criteria of a UAV platform for both Line-Of-Sight (LOS) and Beyond Line-Of-Sight (BLOS) operations. Similar to the substantial efforts carried out by large scale air traffic management programmes including NextGen in US and SESAR in Europe, the Australian airspace is undergoing changes under the OneSky project to incorporate UAV as one of its entities. The general requirements for implementing an effective SAA include:

- The SAA system shall detect both cooperative and non-cooperative collision threats during day and night and considering adverse weather conditions.
- The SAA system shall notify the operator for any imminent collision risk and provide a collision resolution or execute an autonomous avoidance manoeuvre.
- The SAA system shall consider any direction or warning from other avoidance systems.
- The SAA system shall provide a recommended course resume action after any avoidance manoeuvre.

The requirements for autonomous operations include:

- The SAA system shall execute an autonomous avoidance manoeuvre if the pilot does not perform the suggested resolution from the SAA system.
- The SAA system shall provide the operator the necessary information on the progress of the autonomous manoeuvre (time and weather permitting)
- The SAA system shall execute a return-to-course action after an autonomous manoeuvre is executed.

The requirements of separation and avoidance include:

- The UAV SAA system shall warn the operator warnings of obstacles within an estimated distance of 3000 m. In the case of cooperative vehicles the minimum separation shall follow the standards stated by the Federal Aviation Administration (FAA).
- The generated avoidance manoeuvre shall be based in the standards established in FAA 91.113.
- The generated avoidance manoeuvre shall prevent mid-air collision and has to consider other avoidance manoeuvres generated by other systems such as TCAS.

- If the pilot avoidance manoeuvre increases the risk of collision with any other obstacle the system shall override the pilot command.
- If the pilot does not execute a return to course manoeuvre after an avoidance action either from the Flight Control System (FCS) or from the operator, then the UAV shall autonomously return to its original course.

A number of cooperative systems and non-cooperative sensors can be employed in the SAA system design. The non-cooperative SAA sensors are employed to detect intruders or other obstacles in the UAV FOR when cooperative systems are unavailable in the intruders. Optical, thermal, Laser Obstacle Avoidance System (LOAM), Millimetre Wave (MMW) radar, SAR and acoustic sensors can be employed as part of non-cooperative SAA. Moreover, the cooperative systems including TCAS and ADS-B can be combined for with the sensor suite. The SAA technologies are listed in Table 1 representing C for cooperative systems and NC for non-cooperative sensors [20].

TABLE I. SAA CANDIDATES

Sensor/ System	Type	Information	Trajectory
Visual camera	NC, Passive	Azimuth, Elevation	Extracted
Thermal camera	NC, Passive	Azimuth, Elevation	Extracted
LOAM	NC, Active	Range	Extracted
MMW Radar	NC, Active	Range, Bearing	Extracted
SAR	NC, Active	Range, Bearing	Extracted
Acoustic	NC, Active	Azimuth, Elevation	Extracted
ADS-B	C	Position, Altitude and Velocity	Provided
TCAS/ ACAS	C	Range, Altitude	Extracted

Based on the state-of-the-art technologies, a typical Boolean-logic based decision tree SAA system reference architecture is illustrated in Fig. 1. A typical example of prioritisation is selecting ADS-B data when both ADS-B system and TCAS are present on-board the UAV platform (represented by dashed lines in Fig. 1). Considering ADS-B measurements as A, TCAS data as B and the output for cooperative SAA function as O1, the expression for the Boolean logics implementation is derived as follows:

$$O1 = A + (A \oplus T) \quad (1)$$

$$O1 = A + (A\,T' + T\,A') \quad (2)$$

$$O1 = A\,(1 + T') + T\,A' \quad (3)$$

$$O1 = A + T\,A' \quad (4)$$

Similarly, a Boolean logics decision tree is also employed for the non-cooperative case. Representing data from visual camera as V, thermal camera as I, LIDAR as L, MMW radar as M, SAR as S, acoustic as A and the output for non-cooperative SAA function as O2, the expression for the Boolean logics implementation is derived as follows:

$$O2 = A \cdot M \cdot L \cdot S \cdot (V + (V \oplus I)) \quad (5)$$

$$O2 = A \cdot M \cdot L \cdot S \cdot (V + (V\,I' + I\,V')) \quad (6)$$

$$O2 = A \cdot M \cdot L \cdot S \cdot (V + I\,V') \quad (7)$$

A combined decision tree is adopted for accommodating both non-cooperative sensors and cooperative system information. This is described by the overall output O as:

$$O = (O1 \oplus O2) + O2 \quad (8)$$

Additionally, naturally inspired sensors can be form part of the system architecture. Naturally occurring sensory mechanisms derived from behaviours of insects including spatial and temporal isolation, sound as defense, startle and interference, and combining acoustic defences as well as other mechanisms including cognition based sensing can be part of the sensor suite [21-24].

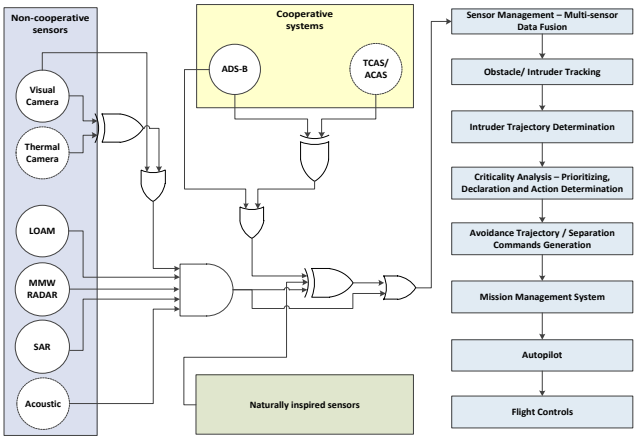

Fig. 1. SAA technologies and system process.

Field Programmable Gate Arrays (FPGA) can be adopted for implementing cooperative system and non-cooperative sensor selecting and sorting through an array of dedicated programmable logic blocks.

III. SAA SYSTEM

The sequential steps involved in the SAA process for executing an efficient Track, Decide and Avoid (TDA) process are illustrated in Fig. 1. The trajectory information of the intruders is determined after performing multi-sensor data fusion techniques [25]. Criticality analysis is performed to prioritize (i.e. to determine if a collision risk threshold is exceeded for all tracked intruders) and to determine the commands to execute an avoidance action. If an evading situation arises, the SAA system generates and optimises an avoidance trajectory according to a priority based cost function based on minimum distance, fuel, time and closure rate criteria with the aid of differential geometry algorithms to generate a smooth and flyable trajectory [26]. In addition to avoiding ground based and airborne obstacles, current

research is also addressing virtual obstacle detection and avoidance including Global Navigation Satellite System (GNSS) unintentional and intentional radiofrequency signal interference (i.e., jamming and spoofing), no-fly zones, noise-sensitive areas and wake turbulence regions.

IV. Uncertainty Analysis

Uncertainty analysis is performed to determine the overall safety volume in the airspace surrounding the intruder track based on SAA Unified Method (SUM). This is accomplished by considering both navigation error of the host UAV platform and tracking error of the intruders/obstacles and translating them to unified range and bearing uncertainty descriptors. Let σ_{Ex}, σ_{Ey} and σ_{Ez} represent standard deviations of the navigation error (σ_{nx}, σ_{ny}, σ_{nz}) or tracking error (σ_{tx}, σ_{ty}, σ_{tz}) in the x, y and z directions respectively. Using a spherical coordinates frame of reference, with origin at the host UAV centre of mass, the range and bearing errors associated with the intruder tracking measurements are transformed into a local Cartesian coordinate frame (either host or intruder body frame). The transformation process results in the generation of navigation and tracking error ellipsoids defined as [3]:

$$\frac{x^2}{{\sigma_{Ex}}^2} + \frac{y^2}{{\sigma_{Ey}}^2} + \frac{z^2}{{\sigma_{Ez}}^2} = 1 \tag{9}$$

(R, θ, φ) are the spherical coordinates defined on a point P. The Cartesian coordinates of the surface points are given by:

$$x_{ij} = R\sin(\theta_i)\cos(\varphi_j) \tag{10}$$

$$y_{ij} = R\sin(\theta_i)\sin(\varphi_j) \tag{11}$$

$$z_{ij} = R\cos(\theta_i) \tag{12}$$

Navigation and tracking error ellipsoids are illustrated in Fig. 2. In order to develop a generalized solution towards obtaining a unified approach to cooperative and non-cooperative SAA, the ellipsoids are subjected to two transforms: rotation, R and translation, T (projection along LOS).

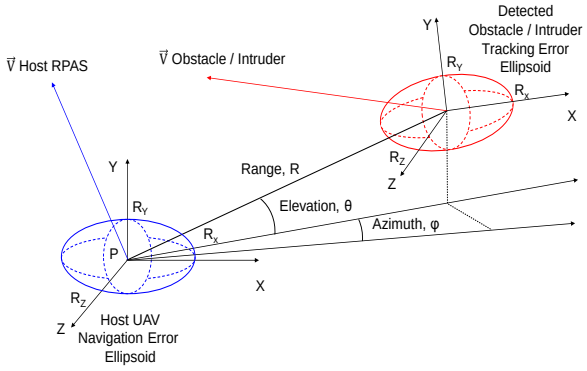

Fig. 2. Navigation and tracking error ellipsoids

The inverse transformation applied to one ellipsoid with respect to another, L is expressed as:

$$L^{-1} = R^{-1}\,T^{-1}L \tag{13}$$

The condition taken into consideration is that the coordinates of the centre, P should satisfy:

$$\frac{x^2}{{(\sigma_{nx}\pm\sigma_{tx})}^2} + \frac{y^2}{{(\sigma_{ny}\pm\sigma_{ty})}^2} + \frac{z^2}{{(\sigma_{nz}\pm\sigma_{tz})}^2} = 1 \tag{14}$$

The simplification of the above equation results considering multivariate Gaussian statistics results in a quadratic condition that is used to derive the miss, tangential and intersection conditions based on the resultant discriminant. Vector analysis is applied to the navigation and tracking ellipsoids. Let $\vec{X}$ denote the points on the surface of the ellipsoid. The components of $\vec{X}$ are X_1 = x, X_2 = y and X_3 = z. Let the surface normal vector be denoted as $\hat{n}$. The normal vector can be expressed as :

$$\hat{n} = \frac{\overrightarrow{X_\theta} \times \overrightarrow{X_\varphi}}{|\overrightarrow{X_\theta} \times \overrightarrow{X_\varphi}|} \tag{15}$$

The differential surface area element, $d\Lambda$ which is an area of a patch of the surface at $r(\theta, \varphi)$ is given by:

$$d\Lambda = S\,d\theta\,d\varphi \tag{16}$$

$$S = \left|\overrightarrow{X_\theta} \times \overrightarrow{X_\varphi}\right| \tag{17}$$

where S is a proportionality constant. The decomposition is expressed in terms of parameters A, B and C given by:

$$A = \overrightarrow{X_\theta}.\overrightarrow{X_\theta} \tag{18}$$

$$B = \overrightarrow{X_\theta}.\overrightarrow{X_\varphi} \tag{19}$$

$$C = \overrightarrow{X_\varphi}.\overrightarrow{X_\theta} \tag{20}$$

The parameters D, E and F are given by:

$$D = -\overrightarrow{X_\theta}.\hat{n}_\theta \tag{21}$$

$$E = \frac{1}{2}\left(\overrightarrow{X_\theta}.\hat{n}_\varphi + \overrightarrow{X_\varphi}.\hat{n}_\theta\right) \tag{22}$$

$$F = -\overrightarrow{X_\varphi}.\hat{n}_\varphi \tag{23}$$

The derivatives of the decomposition of the above parameters are given by:

$$\frac{\delta r(\theta,\varphi)}{\delta\theta} = r_\theta \tag{24}$$

$$\frac{\delta^2 r(\theta,\varphi)}{\delta\theta^2} = r_{\theta\theta} \tag{25}$$

and other derivatives. The parameters D, E and F involve vector products of the derivatives of the components of $\vec{X}$ and $\hat{n}$. S is expressed in spherical harmonic expression as:

$$S = r\left[{r_\varphi}^2 + {r_\theta}^2(\sin\theta)^2 + r^2(\sin\theta)^2\right]^{1/2} \tag{26}$$

The shape of the combined navigation and tracking uncertainty volume (accounting for both uncorrelated or correlated sensor measurements) is conveniently described using spherical harmonics. Let $r(\theta, \psi)$ represent the smooth function defined on the ellipsoid and the parameterization of this spherical harmonic representation is given by:

$$r(\theta,\varphi) = \sum_{l=0}^{\infty}\sum_{m=-l}^{l} X_{lm}\,Y_{lm}(\theta,\varphi) \tag{27}$$

The function $r(\theta, \psi)$ is limited to a number of N finite coefficients and l and m represent the direction index. X_{lm} is a factor and the function $Y_{lm}(\theta, \psi)$ is the spherical harmonic function and is given by:

$$Y_{lm}(\theta, \psi) = \sqrt{\frac{(2l+1)(l-m)!}{4\pi(l+m)!}} P_{lm} \cos(\theta)\, e^{im\psi} \qquad (28)$$

where P_{lm} represents the Legendre functions. The Legendre polynomial function is given by:

$$P_{lm}(x) = \frac{1}{2^n n!} \frac{d^n (x^2-1)^n}{dx^n} \qquad (29)$$

Expanding $e^{im\psi}$ as $C_{lm} \cos(m\psi) + i\, S_{lm} \cos(m\psi)$, we have C_{lm} and S_{lm} defined as the spherical harmonic coefficients. The spherical harmonic coefficients are obtained as:

$$L_{lm} = \{C_{m0},\ S_{lm} \text{and } C_{lm}\} \qquad (30)$$

$$S_{lm} = 0;\ \ l, m\, \varepsilon\, N \qquad (31)$$

$$C_{lm} = 0;\ \ l, m\, \varepsilon\, 2N + 1 \qquad (32)$$

and for all other l, m:

$$C_{lm} = \frac{3}{a^l} \frac{\left(\frac{l}{2}\right)! \left(\frac{l}{m}\right)! (2-\delta_{om})}{2^m (l+3)(l+1)!} \times \sum_{i=0}^{(l-m)/4} \frac{(a^2-b^2)^{(m+4i)/2} [c^2 - \left(\frac{1}{2}\right)(a^2-b^2)]^{(l-m-4i)/2}}{16^i \left(\frac{l-m-4i}{2}\right)! \left(m+\frac{2i}{2}\right)!\, i!} \qquad (33)$$

where δ_{om} is the Kronecker symbol and (a, b, c) represents the semi-major radius of the navigation or tracking error ellipsoid. C_{m0} are the zonal coefficients (functions of latitude) while S_{lm} and C_{lm} are the tesseral coefficients (functions of longitudes). When l=m, sectorial coefficients are obtained which are functions of both latitudes and longitudes. When the errors are correlated tensors analysis is adopted to properly account for covariant or contravariant components. Six components are associated with a rank-2 symmetrical tensor ϕ_{ij}, which are three diagonal and three off-diagonal components usually occurring in pairs. The equation of an ellipsoid associated with the tensor is given by:

$$r_i \phi_{ij} r_j = 1 \qquad (34)$$

where r is the radius vector having components r_i and r_j. Considering a three-dimensional space, the covariance tensor for the error ellipsoid is given as:

$$T = \begin{bmatrix} \phi_{ii} & \phi_{ij} & 0 \\ \phi_{ji} & \phi_{jj} & 0 \\ 0 & 0 & \phi_{kk} \end{bmatrix} \qquad (35)$$

for components (i, j, k) along (X, Y, Z) axes. The partial derivatives of an invariant function provide the components of a covariant vector. A contravariant vector is the same as a contravariant tensor of first order. A notional example of the two combined navigation and tracking error ellipsoids and the resulting uncertainty volume for uncorrelated measurements is illustrated in Fig. 3.

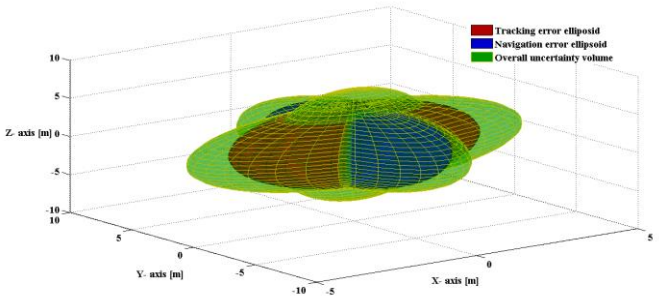

Fig. 3. Uncertainty volume.

The unified approach provides a basis for modelling the avoidance volume surrounding the ground based and airborne obstacles irrespective of the sensors/systems employed on-board the airborne platform. The shape of the overall safety volume is described using harmonic analysis and as a special case, when the errors are correlated, covariant and contravariant tensor theory is applied. The approach grants the possibility of current and future platforms to be equipped with SAA capability based on a sensor-independent and platform-independent solution. The proposed techniques also address the fulfilment of Required Total System Performance (RTSP) for CNS+A framework. This research also addresses the challenges in meeting the stringent GNSS data integrity requirements essential for airworthiness requirements for both cooperative and non-cooperative SAA. Based on a properly designed and certifiable Avionics Based Integrity Augmentation (ABIA) system, an extended spectrum of autonomous and safety-critical operations will be possible, thanks to the continuously monitoring of GNSS integrity levels [27, 28]. This increased level of integrity could facilitate and expedite the pathway to support unrestricted access of RPAS to commercial airspace.

V. Sensor/Systems Algorithms

A. Non-Cooperative sensors

Gimballed visual and thermal cameras are used for determining position and velocity estimates of the obstacles / intruders. In order to effectively use non-cooperative sensors for all-time and all-weather operations, thermal imaging is used in conjunction with the visual sensors. The proposed hardware for the camera provides an approximate FOV of 70º with a resolution of 2.0 MP. The fusion of optical sensors with other non-cooperatives sensors increases the angular accuracy. LIDAR is proposed for extracting range measurements and provides a FOV of 40º in azimuth and 15º in elevation. It allows the operator to select the azimuth orientation of the FOV among three possible directions: aligned with the platform heading (normal flight envelope) or 20º left/right with respect the platform heading. This option provides an optimized coverage for turning manoeuvres at high angular speed. A low-cost navigation

and guidance system is adopted for determining Position, Velocity and Attitude (PVA) estimates, which includes Global Navigation Satellite System (GNSS), Micro-Electromechanical System (MEMS) Inertial Measurement Unit (IMU), Vision Based Navigation (VBN) sensors and Aircraft Dynamics Model (ADM) virtual sensor [21 - 25]. When the set threshold is exceeded and the detection is continuous, high level tracking detection is performed by using a Kalman Filter. The Track-To-Track (T^3) algorithm is employed for sensor fusion. The primary advantage of adopting this method is to combine the estimates instead of combining the observations from different sensors. The track fusion algorithm is defined as the weighted average variance of all the tracks and is given by:

$$\hat{x}_F(k|k) = P_F(k|k) \times \sum_{i=1}^{n} P_i^{-1}(k|k)\, \hat{x}_i\,(k|k) \quad (36)$$

$$P_F(k|k) = [\sum_{i=1}^{n} P_i^{-1}(k|k)]^{-1} \quad (37)$$

There are two main advantages of the track-to-track algorithm against other scan fusion methods:

- At each sensor site there is local independent track information available so a higher integrity is achieved.
- The information needs to be transferred at lower rates for data fusion.

Similar to Extended Kalman Filter (EKF), the track-to-track algorithm assumes a common model of the state. In order to obtain good results for tracking, the system covariance Q and the observation covariance R are considered constant and are assigned with the following values:

$$Q = \begin{bmatrix} 0.1 & 0 & 0 & 0 \\ 0 & 0.1 & 0 & 0 \\ 0 & 0 & 0.1 & 0 \\ 0 & 0 & 0 & 0.1 \end{bmatrix} \quad (38)$$

$$R = \begin{bmatrix} 1 & 0 \\ 0 & 1 \end{bmatrix} \quad (39)$$

It can be observed that compared to a single tracker, the error statistics of the track-to-track algorithm give better results in mean and standard deviation. Once the states are estimated a future trajectory is predicted. The approach employed to do this task is based on an extension of the state and from the output equation:

$$n(k) = Sx(k) \quad (40)$$

where $n = [x\ y\ z]^T$ and the matrix S locates the states in the vector x that belong to the object position and hence we have:

$$\begin{bmatrix} n^{nl}(k+1|k) \\ n^{nl}(k+2|k) \\ \vdots \\ n^{nl}(k+h_p|k) \end{bmatrix} = S \begin{bmatrix} \hat{x}_T(k+1|k) \\ f[\hat{x}_T(k+1|k)] \\ \vdots \\ f[\dots f[\hat{x}_T(k+1|k)] \dots] \end{bmatrix} \quad (41)$$

where h_p is defined as a future horizon up to where it is desired to predict the trajectory. $\hat{x}_T(k+1|k)$ are the estimates of the track-to-track algorithm, that contains information for all the local estimations, at the next sample time. The errors in predicted trajectory can be derived from the quality of the measurements, reflected in the prediction error, which are expressed as:

$$\sigma^2\,(k+\tau|k) = \mathrm{var}[n(k+\tau) - \hat{n}^1(k+\tau|k)] \quad (42)$$

where $n(k+\tau)$ is the exhibited (modelled) trajectory and $\hat{n}^1(k+\tau|k)$ is the predicted optimal trajectory at sample time $k+\tau$. For trajectory prediction, the obstacle centre of mass, the target orientation and the geometric shape of the uncertainty volume are determined. Once the trajectory is predicted, the Risk of Collision (ROC) is determined by calculating the probability of a Near Mid-Air Collision (NMAC) event for the predicted trajectory over the time horizon by employing Monte Carlo approximations given by:

$$P\left(NMAC_{(0,h_p)}\right) \approx \frac{1}{N_{rc}} \sum_{i=1}^{N_{rc}} \left(\min_{0<t_p<h_p} |s_i(t_p)| < d_m\right) \quad (43)$$

where N_{rc} is the number of samples, h_p is defined as a future horizon up to where it is desired to predict the trajectory, d_m is the minimum distance required to avoid the obstacle, t_p is the time horizon defined for collision and the subscript rc is added to distinguish it from the number of runs in a Monte Carlo simulation. The accuracy of the approximation is entirely based on the number of samples.

B. Cooperative systems

Currently the majority of air traffic surveillance around the world is achieved through Primary Surveillance Radar (PSR) as well as Secondary Surveillance Radar (SSR). Automatic Dependent Surveillance Broadcast (ADS-B) has been viewed as a low cost alternative and complement to the current primary surveillance radar. According to the definition provided by International Air Transport Association (IATA), ADS-B refers to the function on a surface vehicle or airplane which broadcasts its state vector together with other relevant information periodically [28]. ADS-B system is used to obtain the state of the intruders. The future position of the intruders is projected based on the estimate of the current state vector and the flight profile. The ADS-B measurement model adopted for intruder position and velocity estimates in x and y cardinal directions is given as:

$$Z(k) = \begin{bmatrix} 1 & 0 & 0 & 0 & 0 & 0 \\ 0 & 1 & 0 & 0 & 0 & 0 \\ 0 & 0 & 0 & 1 & 0 & 0 \\ 0 & 0 & 0 & 0 & 1 & 0 \end{bmatrix} \begin{bmatrix} x \\ \dot{x} \\ \ddot{x} \\ y \\ \dot{y} \\ \ddot{y} \end{bmatrix} + \begin{bmatrix} V_x(k) \\ V_{\dot{x}}(k) \\ V_y(k) \\ V_{\dot{y}}(k) \end{bmatrix} \quad (44)$$

Assuming that the velocity components, $V_x(k)$, $V_{\dot{x}}(k)$, $V_y(k)$ and $V_{\dot{y}}(k)$ are affected only by Gaussian noise with zero mean, the standard deviation is defined by the covariance matrix given by:

$$R = \begin{bmatrix} E[V_x{}^2] & 0 & 0 & 0 \\ 0 & E[V_{\dot{x}}{}^2] & 0 & 0 \\ 0 & 0 & E[V_y{}^2] & 0 \\ 0 & 0 & 0 & E[V_{\dot{y}}{}^2] \end{bmatrix} \quad (45)$$

where E[ ] represents the mean. An Interacting Multiple Model (IMM) algorithm is adopted for data fusion. The IMM model is a state-of-the-art tracking algorithm suitable when multiple kinematic behaviours are to be considered. Using this model, the state vector of the intruders is determined and this is propagated to predict the future trajectories using a probabilistic model. After computing the mixing probability, the combination of the state estimate is given by:

$$\hat{x}_F(k|k) = \sum_{i=j}^{r} \hat{x}^j(k|k)\, \mu_j(k) \quad (46)$$

where $\mu_j(k)$ is the mode probability update. For conflict detection, the resultant covariance matrix, Q after transformation is defined as:

$$Q = R\, S\, R^T \quad (47)$$

where S is the diagonal covariance matrix and R represents the transformation matrix between the heading aligned frame to that of the RPAS host platform frame. The probability of conflict is defined as the volume below the surface of the probability density function, $p(x, y)$ representing the conflict zone. The conflict probability, P_c is expressed as:

$$P_c = \int_{-\Delta y - \Delta yc}^{-\Delta y + \Delta yc} \int_{-\infty}^{+\infty} p(x, y)\, dx\, dy \quad (48)$$

where $\Delta y + \Delta yc$ represents the conflict separation distance and $\Delta xc, \Delta yc$ correspond to the rows of the conflict boundary matrix. The conflict probability is simplified as:

$$P_c = P(-\Delta y + \Delta yc) - P(-\Delta y + \Delta yc) \quad (49)$$

The surveillance data processing is illustrated in Fig. 4.

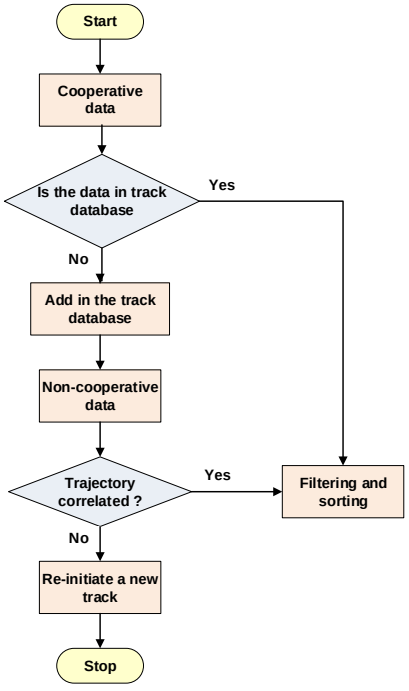

Fig. 4. Surveillance data processing.

Conflict detection and resolution is the collection of the following components:

- Trajectory prediction, which estimates the flight mode of the intruder based on the information derived from cooperative/non-cooperative sensors and predicts the future trajectory of the intruder.
- Conflict detection, calculating the time to separation violation point and conflict probability within the look-ahead time, based on relative range, velocity, and altitude difference.
- Conflict resolution, which uses all available information to resolve the conflicts.
- Monitoring the avoidance manoeuvre, which verifies that conflicts are being resolved as planned.

Conflict detection is based on the geometrical relationship between the intruder and aircraft within the look ahead time based on the state vector information. The violation of minima separation requirement is identified. The information regarding the violation is then transferred to conflict resolution module of the Mission Management System (MMS). After the conflict is resolved, the aircraft nominal trajectory is restored. In terms of speed change resolution, the flight path is the same except for meeting the requirement of time management in the 4D trajectory management. After resolution, navigation computation module of MMS receives inputs from SAA block to compensate the time difference as illustrated in Fig. 5. Additionally, the speed change resolution introduces fewer conflicts during resolving manoeuvre in terms of stochastic analysis because it still flies along its allocated path. Therefore if the speed change resolution is available, it would be preferred compared with other resolutions.

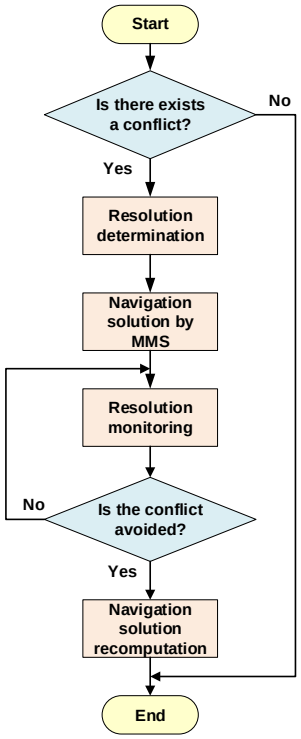

Fig. 5. Interaction with MMS.

VI. Simulation Results

Simulation case studies were performed utilising an AEROSONDE UAV as the host platform. The minimum separation distance was set to d_m = 500 m. The host RPAS was equipped with a SAA system employing cooperative and non-cooperative conflict resolution and collision avoidance. A representative scenario with two intruders was simulated, where intruder 1 (AEROSONDE UAV) was not equipped with cooperative SAA, intruder 2 was equipped with a cooperative SAA system capable of achieving conflict resolution and collision avoidance (large commercial airliner). The intruder states are derived using the host UAV non-cooperative Forward Looking Sensors (FLS) and also tracked with the aid of ADS-B messages (when available). The required separation distance is achieved with respect to all intruders after resolution is performed (both horizontally and vertically). As an example, the horizontal and vertical separation obtained with respect to the first intruder is shown in Fig. 4. The generated avoidance volume and the actual trajectories for this case are shown in Fig. 5.

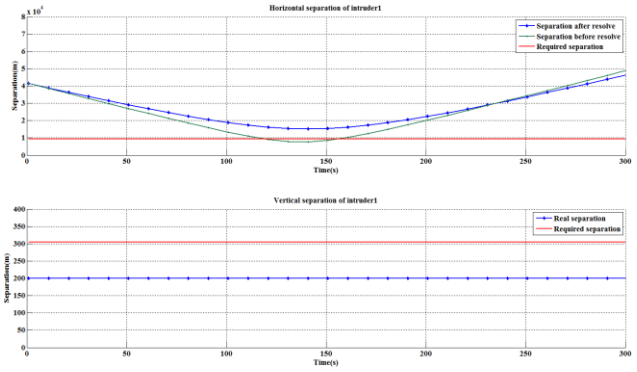

Fig. 4. Intruder 1 horizontal and vertical separation.

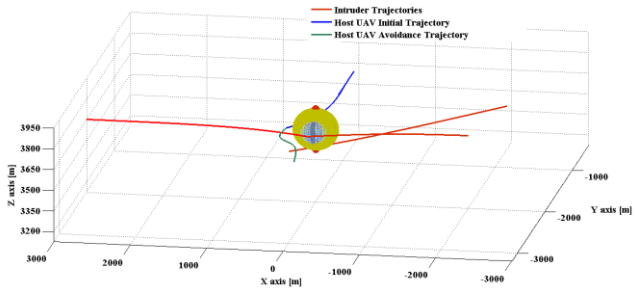

Fig. 5. Avoidance of descending intruder by host UAV.

After the obstacles are detected and tracked, an avoidance trajectory is generated and the corresponding action commands are executed. Results of several simulation cases show that the required safe separation distance is always maintained when the SAA process is performed from ranges in excess of 500 m.

VII. Conclusions

The analytical models describing both non-cooperative and cooperative sensors were discussed. Uncertainty analysis was performed to obtain the overall uncertainty volume associated with the intruder track using a novel unified approach. Various state-of-the-art technologies for DAA were identified and a reference system architecture based on Boolean Decision Logics (BLA) along with the sequential tasks required to implement an effective DAA functionality were presented. A detailed simulation case study was presented and it is concluded that the proposed DAA system is effective when cooperative/non-cooperative detection is performed from ranges in excess of 500 m demonstrating the feasibility of the proposed DAA solution. In future research, integration of the DAA system with other avionics and ground-based systems for Intent Based Operations [29] will be performed.

References

[1] S.P. Cook A.R. Lacher, D.R. Maroney, and A.D. Zeitlin, "UAS Sense and Avoid Development - The Challenges of Technology, Standards, and Certification", 50th AIAA Aerospace Sciences Meeting Including the New Horizons Forum and Aerospace Exposition, Nashville, TN, USA, 2012.

[2] K. Dalamagkidis, K.P. Valavanis, and L.A. Piegl, "On unmanned aircraft systems issues, challenges and operational restrictions preventing integration into the National Airspace System", Progress in Aerospace Sciences, vol. 44, issue 7, pp. 503-519, 2008.

[3] S. Ramasamy, R. Sabatini and A. Gardi, "Towards a Unified Approach to Cooperative and Non-Cooperative RPAS Detect-and-Avoid", Fourth Australasian Unmanned Systems Conference 2014 (ACUS 2014), Melbourne, Australia. DOI: 10.13140/2.1.4841.3764

[4] A. Zeitlin, "Sense and Avoid Evaluations and Standards for Civil Airspace Access" in Unmanned Aircraft Systems, the Global Pperspective, MITRE, pp. 156–7, 2007.

[5] The International Civil Aviation Organization (ICAO), Working Document for the Aviation System Block Upgrades - The Framework for Global Harmonization, Montreal, Canada, 2013.

[6] G. Amato, EUROCAE WG-73 on Unmanned Aircraft Systems, ed: EUROCAE.

[7] JAA, UAV TASK-FORCE Final Report - A concept for European regulations for civil unmanned aerial vehicles (UAVs), 2004.

[8] X. Yu and Y. Zhang, "Sense and Avoid Technologies with Applications to Unmanned Aircraft Systems: Review and Prospects", Progress in Aerospace Sciences, vol. 74, pp. 152-166, 2015.

[9] J. Lai, J.J. Ford, L. Mejias P. O'Shea, and R. Walker, "See and Avoid Using Onboard Computer Vision, Sense and Avoid" in UAS Research and Applications, Plamen Angelov (ed.), John Wiley and Sons, West Sussex, UK, 2012.

[10] S. Ramasamy, A. Gardi and R. Sabatini, "A Laser Obstacle Avoidance System for Manned and Unmanned Aircraft Detect-and-Avoid", Proceedings of the 16th Australian International Aerospace Congress (AIAC16), Melbourne, Australia, February 24, 2015.

[11] A. Finn and S. Franklin, "Acoustic sense & avoid for UAV's", IEEE Intelligent Sensors, Sensor Networks and Information Processing (ISSNIP), Seventh International Conference, 2011.

[12] C.K. Lai, M. Lone, P. Thomas, J. Whidborne, and A. Cooke, "On-Board Trajectory Generation for Collision Avoidance in Unmanned Aerial Vehicles", Proceedings of the IEEE Aerospace Conference, pp. 1-14, 2011. DOI: 10.1109/AERO.2011.5747526

[13] L. Mejias, J. Lai, and T. Bruggemann, "Sensors for Missions", Handbook of Unmanned Aerial Vehicles, pp. 385-399, 2015.

[14] C.G. Prévost, A. Desbiens, E. Ganon, D. Hodouin, "UAV Optimal Obstacle Avoidance while Respecting Target Arrival Specifications", Preprints of the 18th IFAC World Congress, Milano, Italy, pp. 11815-11820, 2008.

[15] P. Cornic, P. Garrec, S. Kemkemian, and L. Ratton, "Sense and Avoid Radar using Data Fusion with Other Sensors", Proceedings of

the IEEE Aerospace Conference, Big Sky, USA, March 2010. DOI: 10.1109/AERO.2011.5747514

[16] Federal Aviation Administration, Pilot's Role in Collision Avoidance, AC90-48C, Washington DC, USA, 1983.

[17] DOT/FAA/CT-96-1, Human Factors Design Guide for Acquisition of Commercial-Off-the-Shelf subsystems, Non-Developmental Items, and Developmental Systems-Final Report and Guide, January 1996.

[18] R. Melnyk, et al. "Sense and Avoid Requirements for Unmanned Aircraft Systems Using a Target Level of Safety Approach", Risk Analysis, vol. 34, issue 10, pp. 1894-1906, 2014.

[19] H.M. Draper, et al. "Human-Machine Interface Development for Common Airborne Sense and Avoid Program", Proceedings of the Human Factors and Ergonomics Society Annual Meeting, vol. 58, no. 1, SAGE Publications, 2014.

[20] S. Ramasamy, R. Sabatini, A. Gardi, "Avionics Sensor Fusion for Small Size Unmanned Aircraft Sense-and-Avoid", IEEE Workshop on Metrology for Aerospace, pp. 271-276, Benevento (Italy), May 2014. DOI: 10.1109/MetroAeroSpace.2014. 6865933

[21] A.L. Miller and A. Surlykke, "How Some Insects Detect and Avoid Being Eaten by Bats: Tactics and Countertactics of Prey and Predator Evolutionarily Speaking, Insects have Responded to Selective Pressure From Bats with New Evasive Mechanisms, and these Very Responses in Turn Put Pressure on Bats to "Improve" Their Tactics", Bioscience, vol. 51, no. 7, pp. 570-581, 2001.

[22] A. Mohamed, S. Watkins, R. Clothier, M. Abdulrahim, K. Massey, and R. Sabatini, "Fixed-wing MAV Attitude Stability in Atmospheric Turbulence—Part 2: Investigating Biologically-inspired Sensors." Progress in Aerospace Sciences, vol. 71, pp. 1-13, 2014.

[23] F.C. Rind, R.D. Santer, and G.A. Wright, "Arousal Facilitates Collision Avoidance Mediated by a Looming Sensitive Visual Neuron in a Fflying Locust", Journal of Neurophysiology, vol. 100, pp. 670-680, 2008.

[24] M.V. Srinivasan, S. Thurrowgood, and D. Soccol, "From Flying Insects to Autonomously Navigating Robots", IEEE Robotics and Automation Magazine, Special Issue on Cognitive Robotics, vol. 16, no. 3, pp. 59-71, 2009.

[25] F. Cappello, S. Ramasamy, and R.Sabatini, "Multi-Sensor Data Fusion Techniques for RPAS Navigation and Guidance", Proceedings of the 16th Australian International Aerospace Congress (AIAC16), Melbourne, Australia, February 24, 2015.

[26] L. Rodriguez, R. Sabatini, S. Ramasamy, and A. Gardi, "A Novel System for Non-Cooperative UAV Sense-And-Avoid", European Navigation Conference (ENC 2013), Vienna, Austria, 2013.

[27] R. Sabatini, T. Moore and C. Hill, "Assessing GNSS Integrity Augmentation Techniques in UAV Sense-and-Avoid Architectures", Proceedings of the AIAC16, Melbourne, Australia, February 24, 2015.

[28] R. Sabatini and G. Palmerini, Differential Global Positioning System (DGPS) for Flight Testing, NATO Research and Technology Organization (RTO) – Systems Concepts and Integration Panel (SCI), AGARDograph Series RTO-AG-160, vol. 21, 2008.

[29] A. Gardi, R. Sabatini, S. Ramasamy and M. Marino, "Automated ATM System for 4-Dimentional Trajectory Based Operations", Proceedings of the 16th Australian International Aerospace Congress (AIAC16), Melbourne, Australia, February 23, 2015.